INTERNATIONAL JOURNAL FOR NUMERICAL METHODS IN FLUIDS, VOL. 10, 327–351 (1990)

A TAYLOR–GALERKIN-BASED ALGORITHM FOR VISCOUS INCOMPRESSIBLE FLOW

D. M. HAWKEN, H. R. TAMADDON-JAHROMI, P. TOWNSEND AND M. F. WEBSTER

Department of Mathematics and Computer Science, University College, Swansea SA2 8PP, U.K.

SUMMARY

In this paper the development and behaviour of a new finite element algorithm for viscous incompressible flow is presented. The stability and background theory are discussed and the numerical performance is considered for some benchmark problems. The Taylor–Galerkin approach naturally leads to a time-stepping algorithm which is shown to perform well for a wide range of Reynolds numbers ($1 \leq Re \leq 400$).* Various modifications to the algorithm are investigated, particularly with respect to their effects on stability and accuracy.

KEY WORDS Finite elements Taylor–Galerkin algorithm Fractional step method Cavity flow

INTRODUCTION

This paper constitutes an interim progress report on the development of the schema presented in Townsend and Webster.[1] There, a primitive variable, finite element algorithm was suggested for transient incompressible viscous flow, adopting a Taylor–Galerkin approach in combination with a fractional step (operator-splitting) method. Such a method was advocated to address the shortcomings of traditional Galerkin methods in the flows of interest and to yield highly accurate methods in the transient context. Attention is given here to establishing the viability of this method for steady two-dimensional Newtonian model problems. The ultimate objective is to simulate transient three-dimensional non-Newtonian flows, but to first gain insight into the behaviour of the algorithm, attention is restricted to this simpler class of problems. Work is however already progressing in more complex regimes. Some successful transient three-dimensional Navier–Stokes computations are now beginning to appear in the literature and indicate the realistic possibilities that are becoming attainable today; see e.g. References 2 and 3.

Literature of relevance here falls into two categories, namely those references that provide solutions to selected model problems and those that have a bearing on the underlying algorithm as of Reference 1. Specific benchmark problems addressed in this paper are variants of the driven cavity problem, namely two cases with different 'top-plate' velocity profiles. Case (a) is for a variable profile where the solution is continuous and is well documented in Peyret and Taylor.[4] Case (b) is for the conventional constant profile, widely reported in the literature, which possesses corner singularities in the solution. Instances of this problem are taken for both low Reynolds number ($Re = 1$) and high Reynolds number ($Re = 400$) under varying conditions. The low-Re range is of interest for highly viscous (diffusion-dominated) flows, whilst high Re values will

* A conventional definition for Re is assumed.

0271–2091/90/030327–25$12.50

Received December 1988
Revised June 1989

provide valuable information on performance for advection-dominated flows. The latter is of particular importance for the viscoelastic context, where the aim is to design schemes which can accommodate highly elastic behaviour and its associated highly convective constitutive component. The methods described will be ideally suited to this task since their origins lie in compressible fluid dynamics, where the equations are of hyperbolic type.

The structure of this paper follows the development of the algorithm through its various stages of successful implementation. First, attention is drawn to a time-stepping scheme which is implicit only in the sense of the presence of the consistent mass matrix that arises naturally in the finite element context. This version, which for clarity is referred to as the *explicit* scheme, enjoyed success at high *Re* but revealed its severe limitations for low *Re*. This knowledge led to the development of an alternative scheme, where the diffusion is treated implicitly and the advection explicitly, and allowed the computation of solutions over a wide range of *Re*. This scheme is referred to as the *implicit* scheme. Consideration is also given to the stability effects caused by the removal of the third fractional step which is associated with incompressibility and its accurate representation. Clearly, once the numerical solution has evolved to an acceptably incompressible steady state, so that this step has a negligible numerical contribution, it is more efficient to discard it altogether. However, the pressure is found to be particularly sensitive to such changes and such practices are shown to invariably destabilize the scheme. Further investigations are pursued into the effects on stability of modifications to step 3, and thus it is shown how stability of the scheme may be enhanced without degrading accuracy (see van Kan[5] for details).

In Reference 1 the explicit time-stepping Taylor–Galerkin algorithm for advection–diffusion was outlined using the same approach as that used to generate Lax–Wendroff difference schemes.[6,7] In fact this scheme closely resembles the two-step Lax–Wendroff scheme proposed by Richtmeyer, which is discussed in Richtmeyer and Morton.[8] A whole family of such schemes is extensively discussed in Reference 4. The merit of explicit schemes generally is that they are efficient and simple to implement, which makes them particularly attractive for the large-scale transient three-dimensional problems that one wishes to attack. Their disadvantage is that they are unstable for large time steps (Δt). Of course there are circumstances, such as in advection-dominated or compressible flows, where Δt may be more constrained by accuracy considerations than by stability. In the present non-linear multidimensional advection–diffusion context there is an absence of a complete theoretical study of stability. Therefore in two dimensions we observe the following practical approximate stability guidelines in our choice of Δt.[4] At low *Re*, Δt is limited by

$$\Delta t \leq h^2/(4Re^{-1} + (|u| + |v|)h), \tag{1}$$

whilst for high *Re*

$$\Delta t \leq h/(|u| + |v|), \tag{2}$$

where (u, v) is the velocity vector and h is a representative value for the mesh spacing.

The literature does contain reference to semi-implicit schemes that adopt an implicit treatment for the diffusion terms.[9] Examples may be found in References 10–12. In this approach only the Courant condition (2) is anticipated to apply, provided that no further constraint arises from the treatment of diffusion.[10] This is true for, say, a Crank–Nicolson choice. Gresho *et al.*[12] demonstrate however that unconditional stability may be attained through this approach for both advection–diffusion and Stokes equations. In their work a balancing tensor diffusivity is employed which is central to their 'upwinding' technique and plays a crucial role in establishing unconditional stability. The two-step Taylor–Galerkin method has similar upwinding goals, and although the implementations differ, one may expect similar behaviour for this method. This is

borne out by considering the combined predictor–corrector doublet to provide the complete step equations in discrete form.[8] The close similarity between the proposed Taylor–Galerkin scheme and the iterative predictor–corrector streamline-upwind Petrov–Galerkin scheme of Brooks and Hughes[10] is also most striking. A crucial factor in favour of the present scheme is that no *ad hoc* problem-dependent parameters are required to achieve this consistent and directionally oriented method.

To extend the schemes of this paper to the Navier–Stokes context a fractional step approach is followed, often referred to as the 'pressure correction or projection' method.[13–16] This was extended to build a second-order time-accurate method. The necessary theoretical background lies in the analysis of van Kan[5] in the finite difference context and of Cuvelier *et al.*[17] for finite elements. This provides a high level of confidence in the overall scheme, confirming consistency and global accuracy, and linearized stability via an energy method. The latter applies in the Stokesian context for an explicit treatment of advection, and hence for insight beyond this regime one must rely on the advection–diffusion analyses quoted above. For Navier–Stokes equations both Quartapelle[11] and Gresho *et al.*[12] have found experimentally that under varying implementations, the stability limitations actually far exceed the Courant condition. Results of the present work indicate that no Δt limit is encountered at low Re, thus providing strong evidence of the acceptability of the implicit approach. This does not appear to be the case for high Re, however, where agreement with the findings in References 11 and 12 is observed.

Below, it is shown how the Galerkin mass matrix equations are solved by employing indirect simple iterative methods. An investigation is conducted into the effect of 'mass lumping' as an alternative to using the consistent mass matrix. This technique abounds in the literatre and is used in the majority of the references cited, yet not without provoking some controversy.[18] The justification for adopting such a technique is mainly on the grounds of economy, though superior stability may result under certain circumstances,[19,20] albeit at the expense of loss in accuracy.[21,22] One is always aware therefore of the deleterious effect such a technique may have on time accuracy, though in the present study one is more concerned with steady state solutions and less with the developing solution history.

Mass lumping is a pragmatic approach of great significance not only in run-time efficiency but also in economy of evaluation effort. For example, one may observe this in the evaluation of the matrix in the discrete Poisson equation for pressure.[13] This latter issue is avoided here by virtue of the order of temporal and spatial discretization involved. Note also that taking a finite difference discretization is in some sense equivalent to mass lumping. Past experience has shown that mass lumping always provides superior stability qualities with no significant accuracy discrepancies in the steady state solution. However, since the major cost per time step is centred around the evaluation of right-hand-side vectors and not the iterative solution phases, one concludes to date that the increased overall number of time steps required when using mass lumping is in certain circumstances actually less cost-effective than would otherwise be the case. Comments on this issue are made in the sections containing the numerical results.

EXPLICIT TIME-STEPPING SCHEME

Algorithmic development

Adopting the notation and conventions of Reference 1, the incompressible Navier–Stokes equations in the absence of body forces, are given by

$$\rho \mathbf{u}_t = \mu \nabla^2 \mathbf{u} - \rho \mathbf{u} \cdot \nabla \mathbf{u} - \nabla p, \tag{3}$$

$$\nabla \cdot \mathbf{u} = 0, \tag{4}$$

where ∇^2 is the Laplacian and ∇ the gradient operator, ρ is the density, μ is the viscosity, $\mathbf{u}$ is the velocity vector and p is the pressure. Boldface type is used to represent vectorial quantities, the subscript is used to denote differentiation with respect to time, and appropriate boundary and initial conditions are assumed.

A semidiscrete Galerkin spatial formulation is adopted, leading to approximations $U(\mathbf{x}, t)$ and $P(\mathbf{x}, t)$ to the velocity and pressure fields respectively, where

$$U(\mathbf{x}, t) = U_j(t)\phi_j(\mathbf{x}), \qquad P(\mathbf{x}, t) = P_j(t)\psi_j(\mathbf{x}). \tag{5}$$

Then $\mathbf{U}$ and $\mathbf{P}$ represent the time-dependent vectors of nodal values of velocity and pressure with components U_j and P_j, and ϕ_j and ψ_j are the respective basis functions spanning the appropriate trial spaces. Here ϕ_j are selected as piecewise quadratics and ψ_j as piecewise linears on triangles.

In Reference 1 the two-step Taylor–Galerkin method was introduced to solve 1D first-order evolutionary hyperbolic equations. This provides the simple and effective mechanism by which the system Jacobian can be evaluated via a predictor–corrector doublet over a single time step. Extensions to higher spatial dimensions, and to instances where second-order differential (diffusive) terms arise, can then be handled in a straightforward manner. This naturally leads to solving systems of equations governed by the Galerkin mass matrix which is discussed in the next section.

Consideration was then given to the Navier–Stokes equations involving the additional complications of incompressibility and the introduction of the pressure term in the momentum equations. The projection method was considered appropriate here. This was developed to second-order time accuracy and introduced some new features. These include solving for the pressure difference over a time step as a primary variable in a Poisson equation; requiring the provision of a consistent initial condition for pressure; and the introduction of an intermediate free variable $\mathbf{U}^*$ to be associated with a non-divergence-free velocity vector. The numerical treatment of the associated boundary and initial conditions could then be achieved simply and accurately.

With only minor modifications from Reference 1, the explicit Taylor–Galerkin scheme in fully discrete matrix form now reads

$$\text{step 1a} \quad 2\frac{\rho}{\Delta t}\mathbf{M}(\mathbf{U}^{n+1/2} - \mathbf{U}^n) = \{\mathbf{F} - [\mu\mathbf{S} + \rho\mathbf{N}(\mathbf{U})]\mathbf{U}\}^n + \mathbf{L}^{\mathrm{T}}\mathbf{P}^n, \tag{6a}$$

$$\text{step 1b} \quad \frac{\rho}{\Delta t}\mathbf{M}(\mathbf{U}^* - \mathbf{U}^n) = \{\mathbf{F} - [\mu\mathbf{S} + \rho\mathbf{N}(\mathbf{U})]\mathbf{U}\}^{n+1/2} + \mathbf{L}^{\mathrm{T}}\mathbf{P}^n, \tag{6b}$$

$$\text{step 2} \quad \theta\mathbf{K}\mathbf{Q}^{n+1} = -\frac{\rho}{\Delta t}\mathbf{L}\mathbf{U}^* \tag{6c}$$

$$\text{step 3} \quad \frac{\rho}{\Delta t}\mathbf{M}(\mathbf{U}^{n+1} - \mathbf{U}^*) = \theta\mathbf{L}^{\mathrm{T}}\mathbf{Q}^{n+1}, \tag{6d}$$

where n denotes the time step index, $\mathbf{Q}^{n+1} = \mathbf{P}^{n+1} - \mathbf{P}^n$, $\mathbf{M}$ is the consistent mass matrix, $\mathbf{S}$ is the 'diffusion' matrix, $\mathbf{N}$ is the 'advection' matrix, $\mathbf{K}$ is the pressure stiffness matrix, $\mathbf{F}$ is the forcing function vector due to boundary conditions and $\mathbf{L}$ is the matrix that arises from incompressibility. For second-order accuracy in time the Crank–Nicolson choice of $\theta = 0{\cdot}5$ is adopted. The inclusion of the half-step within the first fractional step characterizes the extension of first-order projection methods to second-order Taylor–Galerkin/projection methods. For reasons of resolution, it is appropriate to take an integration by parts on the right-hand side at step 3 and hence recast the differential operator onto the quadratic test functions for velocity. With the afore-

mentioned treatment of boundary conditions as in Reference 1, no further modifications to the scheme are necessary.

At step 2 the Poisson equation for the pressure difference arises where the constant stiffness matrix **K** has a symmetrical banded structure. This is solved per time step by a direct Choleski method, requiring a single reduction phase at the outset and a back-substitution phase at each time step. This is fortuitous since the arithmetic operation count is $m_p \times b \times (b + 1)/2$ for the former and outweighs $m_p \times 2b$ for the latter, where m_p is the number of nodal pressure unknowns and b is the half-bandwidth of **K**.[23] Overall, this leads to an algorithm with $O(m_v)$ memory space and $O(m_v)$ run-time worst-case complexities in the maximum number of nodal unknowns per variable, m_v (see Aho *et al.* for definitions[24]). Of course, for run-time complexity the constant of proportionality will depend on, amongst other things, the number of time steps involved. The run-time complexity per time step is in fact linearly dependent on both the number of nodal unknowns and the number of elements, m_e, in the mesh. The constants of proportionality dictate which factor will dominate in practical implementations. Here all matrix–vector multiplications are performed in an element-wise manner and nodal calculations occur in solution phases throughout steps 1–3. Currently, the predominance of computation is within right-hand-side vector calculations, particularly so at step 1. Hence, since m_v is $O(m_e)$, the run-time complexity is more appropriately expressed as $O(m_e)$.

Through the use of simplex elements, considerable economic benefits may be derived in terms of cost and efficiency by replacing quadrature with exact integration wherever this is possible. Furthermore, there are no apparent numerical differences in the associated solutions that are derived from either approach. Since most modern codes avoid element level storage of information and simply recompute such values, this is a significant factor to consider. Past experience indicates that run-time cost may be practically halved by adopting such analytic integration techniques.

Treatment of the Galerkin mass matrix equations

At steps 1 and 3 of the algorithm one must solve a system of equations for an unknown difference vector **X** over a time step of the form

$$\mathbf{MX} = \mathbf{b}, \tag{7}$$

where **M** is the mass matrix and information carried in the vector **b** is known at each solution stage. Hence one requires the inversion of the mass matrix. Direct inversion is avoided for reasons of economy in computer storage and cost efficiency. To take advantage of modern computer hardware developments it is important to extract parallelism from the algorithm. One way to accomplish this is to use iterative methods of solution and to uncouple the individual velocity components so that each may be treated independently. A single component then constitutes a typical vector **X** of nodal point values over the domain.

Again for reasons of economy, the consistent mass matrix is never actually assembled. Instead only the element contributions are used in a simple, Jacobi iteration. Thus there is no storage overhead for the consistent mass matrix. The mass matrix is symmetric positive-definite with a banded structure, and iterative methods are known to be appropriate for the solution of such Galerkin mass matrix equations when diagonally preconditioned. For example, the conjugate gradient method gives extremely rapid convergence at a rate that is independent of the mesh size (*number of nodal unknowns*) and, for simplex elements, even the element shapes.[25] For the Jacobi iteration, rapid convergence in a handful of iterations is the expected norm for steady problems.[26]

The basic iteration is defined in terms of the splitting of $\mathbf{M}$ about a chosen diagonal form $\mathbf{M}_d$ as follows:

$$\mathbf{M}_d\mathbf{X}^{(r+1)} = (\mathbf{M}_d - \omega\mathbf{M})\mathbf{X}^{(r)} + \omega\mathbf{b}, \tag{8}$$

where r is the iteration number and ω is a positive relaxation factor. For the conventional Jacobi method $\omega = 1$, otherwise the iteration is the extrapolated Jacobi method.[27] This provides an iteration matrix of the form $\mathbf{I} - \omega\mathbf{M}_d^{-1}\mathbf{M}$ and a method that is symmetrizable and hence amenable to various iterative acceleration techniques in the terminology of Hageman and Young.[28] Justification for iteration (8) may be found in the approximate factorization analysis for $\mathbf{M}^{-1}$ presented by Donea *et al.*[29] There it is shown how *three* passes of such an iteration are equivalent to a three-term truncated approximation series to $\mathbf{M}^{-1}$. The assumption that $\|\mathbf{M}_d^{-1/2}\mathbf{M}\mathbf{M}_d^{-1/2} - \mathbf{I}\|_2 < 1$ is equivalent to the requirement that the spectral radius of the iteration matrix be less than unity, which is also necessary for iterative convergence.

Of necessity one must store the vectorial form of $\mathbf{M}_d$ and a vanishing initial guess is always assumed. This provides a very good initial guess if the problem is slowly changing in time or if the time step is sufficiently small.[28] Clearly one such iteration is equivalent to replacing the consistent mass matrix with the diagonal matrix $\mathbf{M}_d$ and hence also to mass lumping if $\mathbf{M}_d$ is chosen suitably. Various choices of $\mathbf{M}_d$ have been tried. The trivial diagonal choice $\mathbf{M}_{d1}$, though yielding linear convergence rates, did not perform well in the sense that it was found to induce instabilities through the time steps in certain flow situations (typically where free boundary conditions were involved). Therefore this choice was abandoned in favour of the more commonly used row sum* form $\mathbf{M}_{d2}$. This choice was found to be particularly appropriate, giving rapid convergence rates, with acceptable convergence being achieved in at most three to five such iterations.

The analysis of Wathen provides upper and lower bounds for the eigenvalues of $\mathbf{M}_{d1}^{-1}\mathbf{M}$. For example, with quadratic basis functions an upper bound is given by $\lambda_{max} \leq 2{\cdot}0598$ and a lower bound is $\lambda_{min} \geq 0{\cdot}3924$. The required condition for the Jacobi method to converge is $\lambda_{max} < 2$, whilst for the extrapolated Jacobi method the condition is $\omega\lambda_{max} < 2$. Upper and lower bounds for the eigenvalues of $\mathbf{M}_{d2}^{-1}\mathbf{M}$ follow similarly and are found to be 0·971 88 and 0·185 95 respectively, being about half the values of those for the $\mathbf{M}_{d1}^{-1}\mathbf{M}$ case as anticipated. Hence it is not surprising that the row sum version works so well and clearly results in a convergent Jacobi method with $\omega = 1$. Alternatively, with $\mathbf{M}_{d1}$, ω must be less than 0·970 98 to guarantee convergence.

In certain instances the optimal condition number and hence the convergence rate may be predicted from attainable upper and lower eigenvalue bounds and through a suitable choice of ω. To illustrate this for the $\mathbf{M}_{d1}$ option, ω_{opt} is 0·9 precisely for linear elements, whilst for quadratic elements ω_{opt} is approximately 0·815 6 (if one presumes that the upper and lower eigenvalue bounds of Wathen are closely attained). Optimal values for the $\mathbf{M}_{d2}$ case are found similarly, and for quadratic elements ω_{opt} is approximately 1·7274, a value which is reflected in numerical experiments. However, empirical evidence to date indicates that the attainment of optimal iteration parameters is not a critical issue in the present calculations, where one is mainly interested in using the iterative procedure at each time step merely as a vehicle to reach steady state. In fact the main results of this article were produced with $\omega = 1$. The convergence rate in the early iterations on each occasion the iteration is invoked is what matters here. Recent evidence would indicate that iteration (8) is superior in this respect over a conjugate-gradient-accelerated iteration when the latter is implemented with either the $\mathbf{M}_{d1}$ or $\mathbf{M}_{d2}$ choice.

---

* In modulus for quadratic elements with negative element matrix coefficients.

Numerical results for the explicit scheme

A thorough study of the cavity flow problem under profile case (a) is now described. Solutions for the constant profile case (b) problem are included at the appropriate station as they arise. This section concentrates on the results for the explicit scheme where the histories of the relative error norms are displayed for velocity and pressure in both L_2- and L_∞-measures and are defined as

$$E = \|\mathbf{X}^{n+1} - \mathbf{X}^n\| / \|\mathbf{X}^n\| \tag{9}$$

in the underlying respective norm. The notation adopted is $+$, $\times$ for velocity and $\square$, $\boxplus$ for pressure in the L_2- and L_∞-norms respectively. This choice is made because these measures provide sensitive indicators of overall algorithmic performance. Where relevant, development histories of velocity magnitudes at selected domain points as a function of time steps are presented as *insets* on relative error norm plots. The two meshes employed for the different levels of refinement are illustrated in Figure 1. These meshes possess the superconvergence property (except the isolated central region[30]) and have corner regions which are not locked by the boundary conditions. Some investigation with exponentially graded meshes and also meshes with 'locking' corners was conducted and the proposed meshes of Figure 1 proved a superior option.

High-Re range. The results for $Re = 400$ are displayed in Figures 2–4. Here attention is directed to the effect of switching off the third step of the algorithm when a suitably incompressible velocity field has been reached (see Figure 2). Clearly this induces instabilities in the relative error norms for pressure of a periodic, oscillatory and decaying form. The level of pressure is so large that it is off the scale in Figure 2(b). The necessity to retain this third step is therefore established, if only for its numerical role. The acceptable level of the time step is of note and the large number of time steps necessary is typical of high-Re simulations. In this case, whilst the number of mass iterations remained fixed, taking a smaller time step had little effect, as seen in Figures 3(a) and 3(b).

The effects of altering the number of mass iterations can be observed in Figures 3(c) and 3(d). The case with only one mass iteration is completely smooth in the monitored relative error norms throughout the evolution process, but the solution history development has underachieved that which the five- or three-iteration alternatives provide. After 250 time steps the level of reduction is about 30%. The same ultimate steady state is reached for all variants, but the relative time cost is in favour of the three-iteration version. Increasing the number of mass iterations from three to five at fixed Δt seems to have little effect after the start-up phase, where larger fluctuations in both amplitude and frequency are always observed at the higher iteration numbers. Here three iterations appears to be quite acceptable, providing a sensible balance between cost and precision.

The steady state solutions in velocity vector plot, streamfunction, pressure and velocity components across the centrelines of the cavity are presented in Figures 4(a) and 4(b) for problem cases (a) and (b) respectively. Tables I(a) and I(b) contain the associated details of vortex centre position and strength, $(u_{\max}, v_{\max})$ on centreline, comparisons against the literature and also across the variety of numerical schemes discussed in this paper. To suit convention, $u_{\max}$ is reported with positive sign. The results are for two characteristic mesh element sizes of $h = 0{\cdot}1$ and $0{\cdot}05$ (taken over element widths) and indicate the high level of spatial accuracy of the present schemes, confirming convergence to the accepted steady state solution. Note also that the streamfunction is interpolated by linear trial functions for convenience, being recovered from the highly accurate velocity solution. Hence a slight degradation in accuracy must be anticipated in the streamfunction. Concerning the literature, the basis for comparison is one of numerical results only for the present model problems.

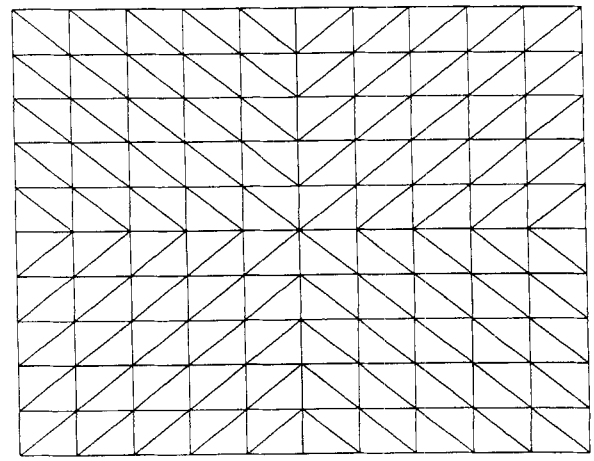

Figure 1(a). Cavity mesh ($h = 0{\cdot}1$)

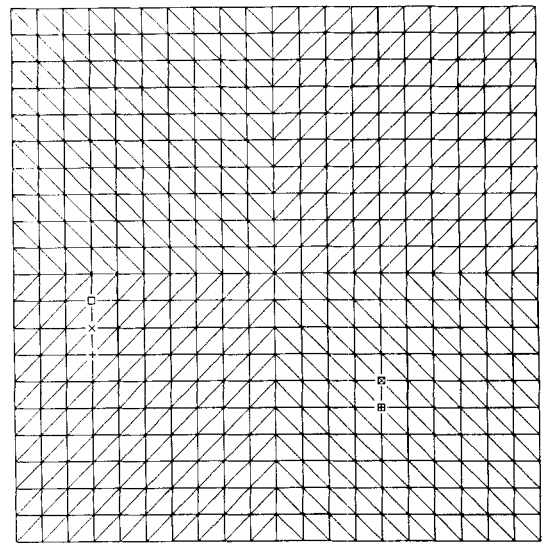

Figure 1(b). Cavity mesh ($h = 0{\cdot}05$): + (0·15, 0·35), × (0·15, 0·4), □ (0·15, 0·45), ⊞ (0·7, 0·25), ⊠ (0·7, 0·3)

Low-Re range. The corresponding results for $Re = 1$ are presented in Figure 5. Switching off step 3 has the same influence here as for high *Re*, as seen in Figures 5(a) and 5(b). The larger range in scale in Figure 5(a) is used to reflect the requirements to reach the steady state. Note again that the pressure plot has disappeared off the scale in Figure 5(b). The value of the time step, $\Delta t = 0{\cdot}000\,03$, is seen to be particularly small which therefore incurs a large number of steps. This is generally an unacceptable penalty to pay compared with conventional diffusion-based schemes at this low *Re* level.

The effects of altering the number of mass iterations can be seen in Figures 5(a) and 5(c). The decrease in the number of mass iterations from five to one has the same response as before. For the one-iteration case the relative error norms are smooth throughout their development, though

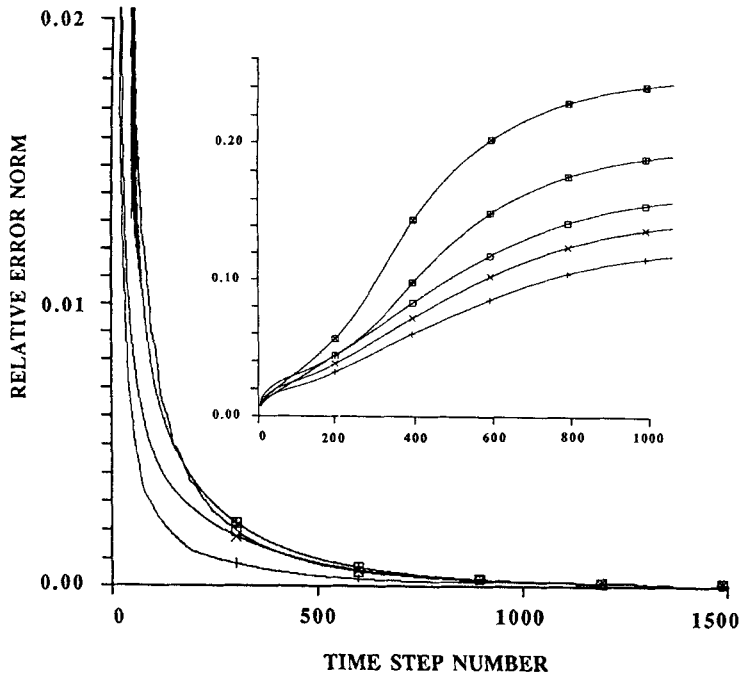

Figure 2(a). Effect of stage 3: present ($Re = 400$, $\Delta t = 0{\cdot}02$, 3 iterations, explicit scheme)

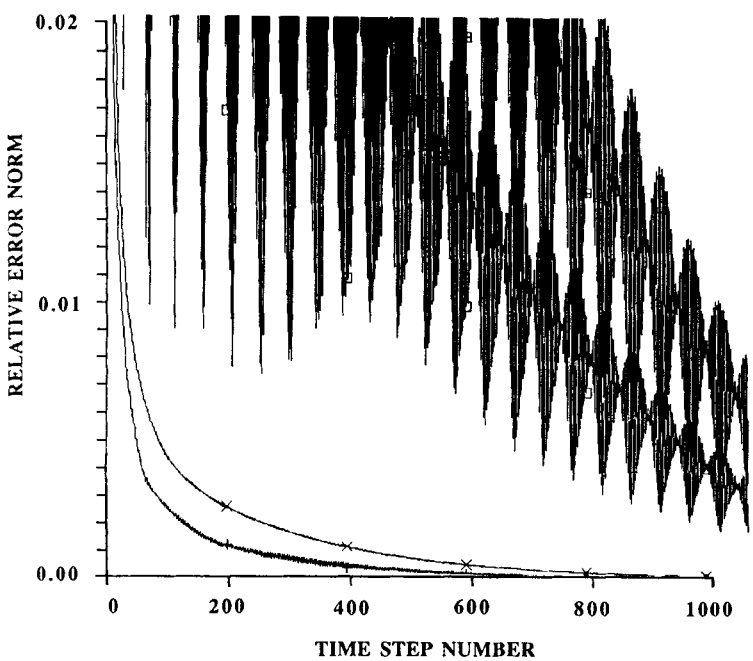

Figure 2(b). Effect of stage 3: removed ($Re = 400$, $\Delta t = 0{\cdot}02$, 3 iterations, explicit scheme)

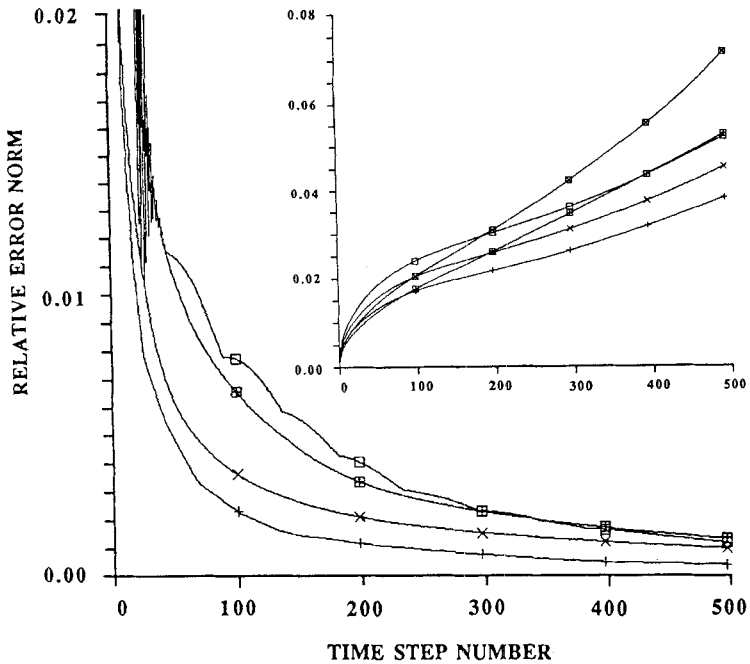

Figure 3(a). Effect of time step: $Re = 400$, $\Delta t = 0{\cdot}01$, 3 iterations, explicit scheme

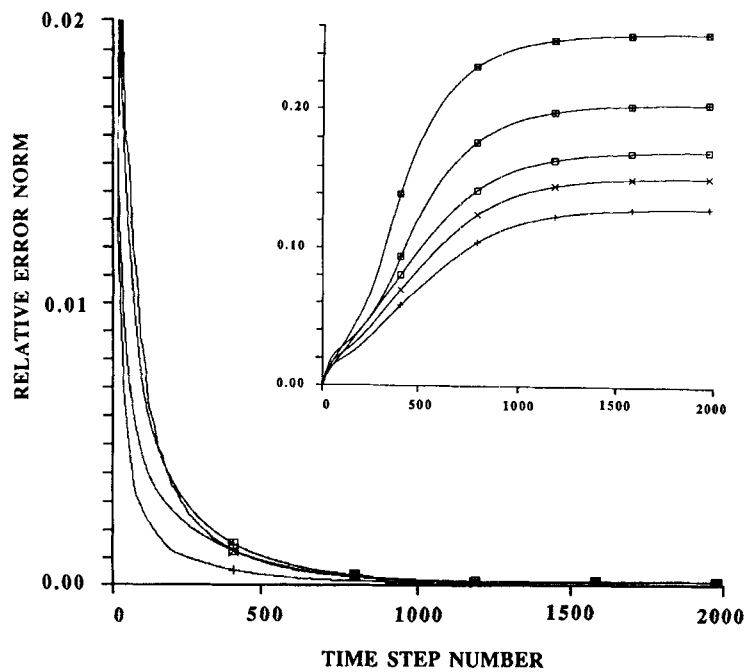

Figure 3(b). Effect of time step: $Re = 400$, $\Delta t = 0{\cdot}02$, 3 iterations, explicit scheme

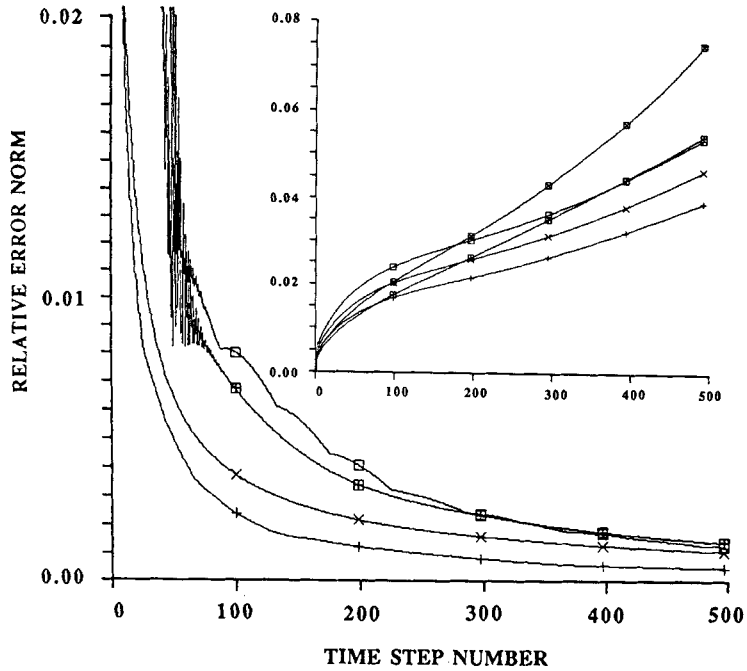

Figure 3(c). Effect of mass iteration number: $Re = 400$, $\Delta t = 0{\cdot}01$, 5 iterations, explicit scheme

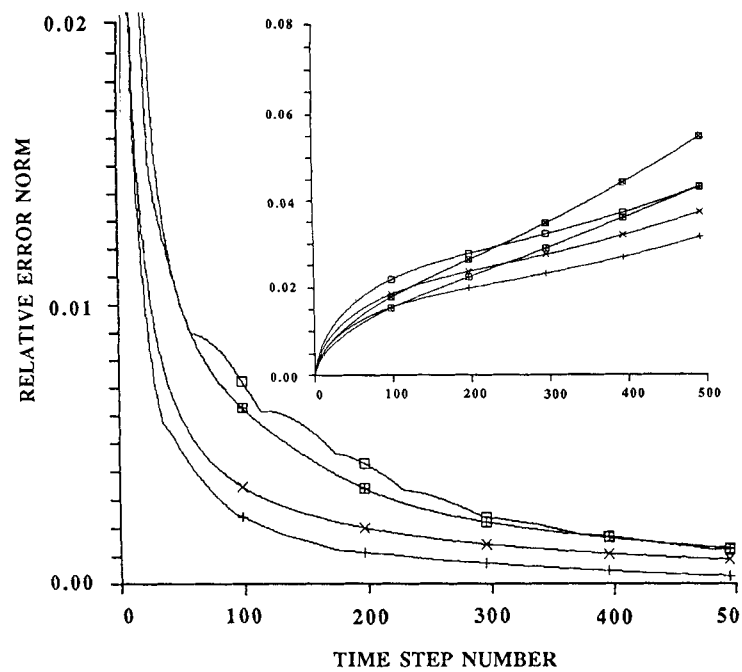

Figure 3(d). Effect of mass iteration number: $Re = 400$, $\Delta t = 0{\cdot}01$, 1 iteration, explicit scheme

again after 250 time steps the solution has underachieved that which the five- or three-iteration alternatives provide by about 10%. The solution history developments for the higher iteration numbers are insensitive to switching off the third fractional stage and may be observed in Figure 5(b). Again it is preferable to elect for a larger number of iterations; in this case the three-iteration option appears optimal and hence the appropriate choice for the *explicit* scheme under all circumstances reported.

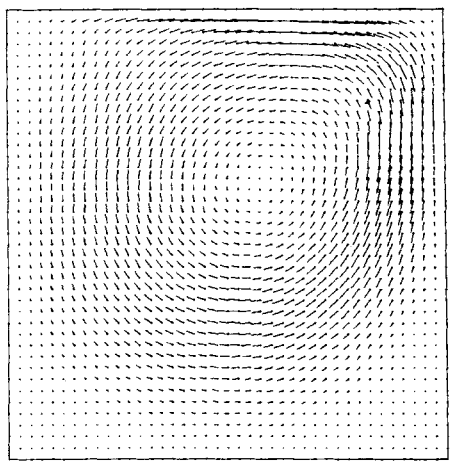

(i)

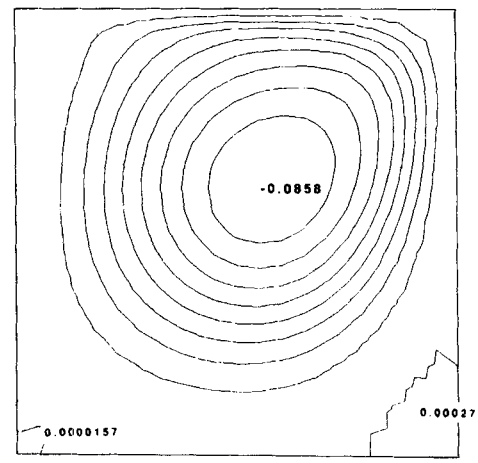

(ii)

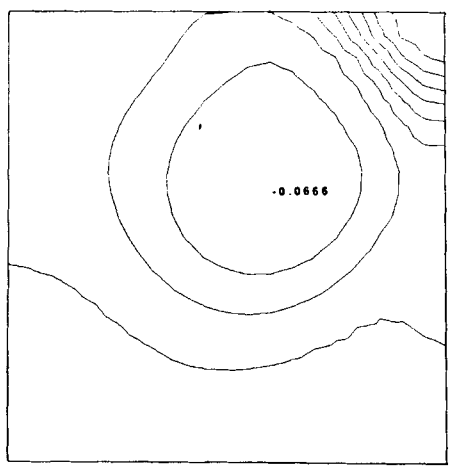

(iii)

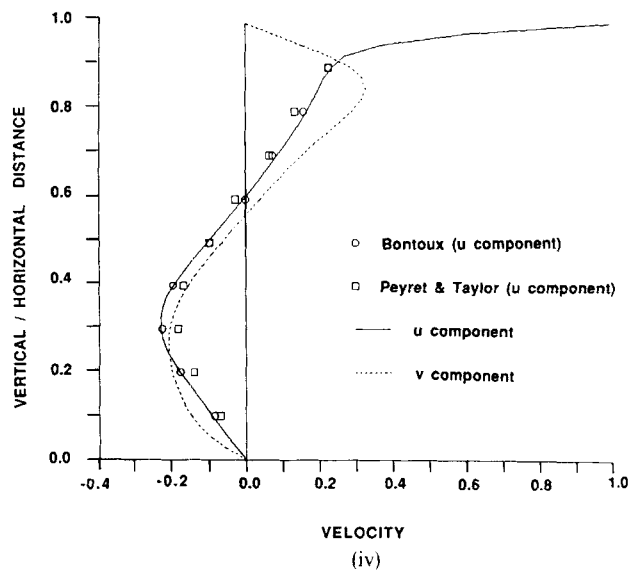

(iv)

Figure 4(a). Steady state solution case (a): $Re = 400$, $\Delta t = 0{\cdot}02$, 3 iterations, explicit scheme. (i) Velocity field; (ii) streamfunction contours; (iii) pressure contours; (iv) velocity profiles ($u(0{\cdot}5, y)$ and $v(x, 0{\cdot}5)$)

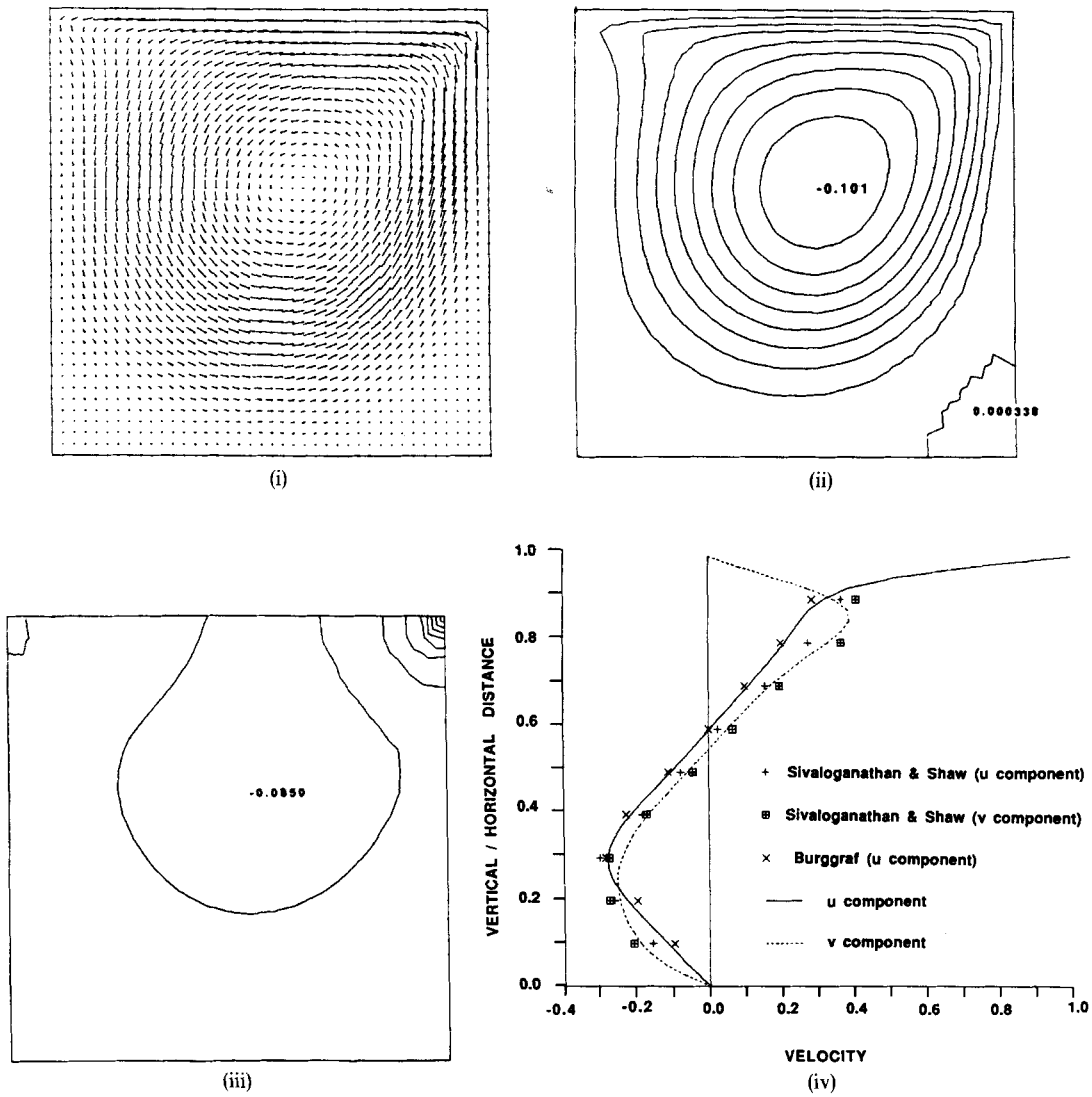

Figure 4(b). Steady state solution case (b): $Re = 400$, $\Delta t = 0{\cdot}02$, 3 iterations, explicit scheme. (i) Velocity field; (ii) streamfunction contours; (iii) pressure contours; (iv) velocity profiles ($u(0{\cdot}5, y)$ and $v(x, 0{\cdot}5)$)

Table Ia. Comparison of steady state solution against the literature: case (a), $Re = 400$

Scheme	h	ψ_{vc}	Vortex centre	$U_{max}(0{\cdot}5, y)$	$V_{max}(x, 0{\cdot}5)$	$V_{min}(x, 0{\cdot}5)$
Explicit	0·05	0·0858	(0·45, 0·60)	0·233	0·336	−0·214
Explicit	0·10	0·0877	(0·45, 0·60)	0·242	0·345	−0·215
Implicit	0·05	0·0855	(0·45, 0·60)	0·233	0·329	−0·211
Implicit	0·10	0·0877	(0·45, 0·60)	0·242	0·340	−0·214
Reference 31	0·06	0·0577	(0·38, 0·62)	—	—	—
Reference 4	0·05	0·0750	(0·40, 0·65)	0·188	—	—
Reference 32	0·05	0·0844	(0·40, 0·65)	0·229	—	—

Table Ib. Comparison of steady state solution against the literature: case (b), $Re = 400$

Scheme	h	ψ_{vc}	Vortex centre	$U_{max}(0{\cdot}5, y)$	$V_{max}(x, 0{\cdot}5)$	$V_{min}(x, 0{\cdot}5)$
Explicit	0·050	0·1012	(0·45, 0·60)	0·285	0·390	−0·250
Implicit	0·050	0·1014	(0·45, 0·60)	0·285	0·390	−0·250
Reference 33	0·050	0·0675	(0·35, 0·73)	—	—	—
Reference 33	0·025	0·1017	(0·44, 0·61)	0·285	—	—
Reference 34	0·050	0·1064	—	—	—	—
Reference 35	0·020	0·1014	(0·45, 0·60)	0·210	—	—
Reference 36	0·031 × 0·062	0·11363	(0·55463, 0·60415)	—	—	—
Reference 37	0·00714	0·11297	(0·55714, 0·60714)	—	—	—
Reference 38	0·015	0·112	(0·44, 0·62)	0·300	0·450	−0·293

IMPLICIT TIME-STEPPING SCHEME

Algorithmic development

By adopting a Crank–Nicolson representation for the diffusion terms, but otherwise retaining the predominantely explicit approach as before, the following fully discretized Galerkin equations may be derived:

$$\text{step 1a} \quad \left(\frac{2\rho}{\Delta t}\mathbf{M} + \frac{\mu}{2}\mathbf{S}\right)(\mathbf{U}^{n+1/2} - \mathbf{U}^n) = \tfrac{1}{2}(\mathbf{F}^n + \mathbf{F}^{n+1/2}) + \{-[\mu\mathbf{S} + \rho\mathbf{N}(\mathbf{U})]\mathbf{U} + \mathbf{L}^{\mathrm{T}}\mathbf{P}\}^n, \tag{10a}$$

$$\text{step 1b} \quad \left(\frac{\rho}{\Delta t}\mathbf{M} + \frac{\mu}{2}\mathbf{S}\right)(\mathbf{U}^* - \mathbf{U}^n) = \tfrac{1}{2}(\mathbf{F}^{n+1} + \mathbf{F}^n) + (-\mu\mathbf{S}\mathbf{U} + \mathbf{L}^{\mathrm{T}}\mathbf{P}\}^n - [\rho\mathbf{N}(\mathbf{U})\mathbf{U}]^{n+1/2}, \tag{10b}$$

$$\text{step 2} \quad \theta\mathbf{K}\mathbf{Q}^{n+1} = -\frac{\rho}{\Delta t}\mathbf{L}\mathbf{U}^*, \tag{10c}$$

$$\text{step 3} \quad \left(\frac{\rho}{\Delta t}\mathbf{M} + \frac{\mu}{2}\mathbf{S}\right)(\mathbf{U}^{n+1} - \mathbf{U}^*) = \theta\mathbf{L}^{\mathrm{T}}\mathbf{Q}^{n+1}. \tag{10d}$$

$$\uparrow$$

Note that for time-independent boundary conditions, $\mathbf{F}^n = \mathbf{F}^{n+1/2} = \mathbf{F}^{n+1}$. The arrow below step 3 is used to highlight a particular term which comes from a consistent derivation. Its omission is found not to hinder consistency and furthermore enhances stability of the overall scheme. This amounts to discarding a term of the form $\Delta t\mu\mathbf{S}(\mathbf{U}^{n+1} - \mathbf{U}^*)/2$.[22] Major difficulties arise however when this term is retained: then higher-order differentials result in the derivation at step 2 which are difficult to resolve with the present finite element technique and a choice of C^0 trial functions. Therefore such contributions at step 2 are presently ignored.

The new form of the iteration matrix that results from this scheme does not alter the attractive convergence behaviour achieved with the mass matrix alone. This is largely due to the dominance of the mass matrix contribution by virtue of the Δt scaling, a fact that is borne out in practice. It is of note that $\mathbf{S}$ is a symmetric positive-semidefinite matrix and again possesses a strongly banded structure. For large Re values the diffusive contributions to the new scheme become negligible and hence the explicit and implicit forms become synonymous. The iteration matrix is then

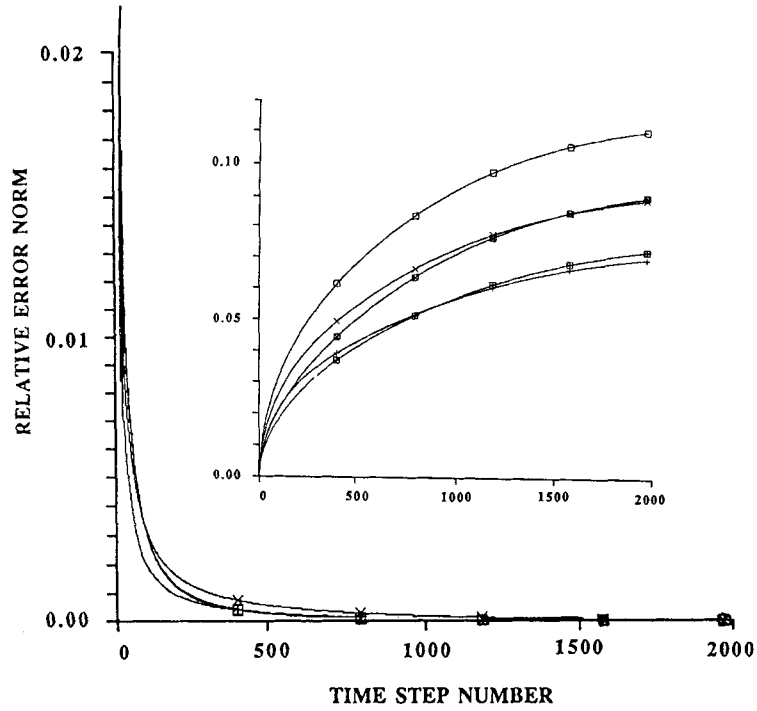

Figure 5(a). Effect of stage 3: present ($Re = 1$, $\Delta t = 0{\cdot}000\,03$, 5 iterations, explicit scheme)

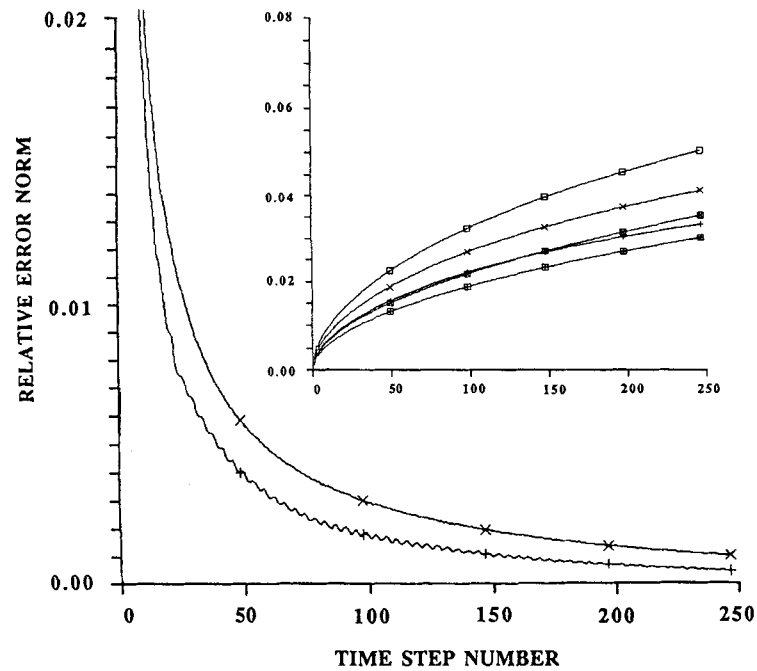

Figure 5(b). Effect of stage 3: removed ($Re = 1$, $\Delta t = 0{\cdot}000\,03$, 5 iterations, explicit scheme)

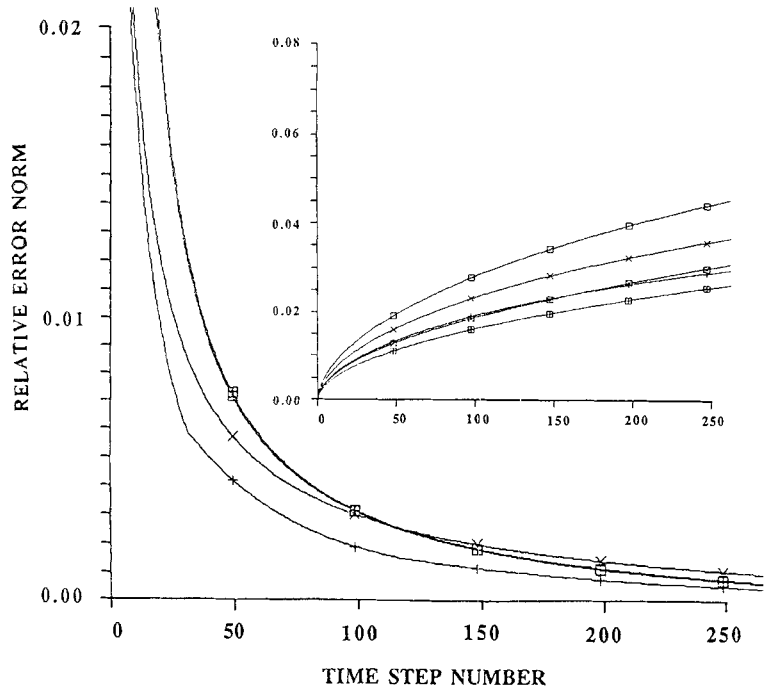

Figure 5(c). Effect of mass iteration number: $Re = 1$, $\Delta t = 0{\cdot}000\,03$, 1 iteration, explicit scheme

dominated by the presence of the mass matrix. For low *Re*, stability constraints are evidently of no consequence since an upper limit on Δt is not encountered. Conversely, for large *Re*, an order-of-magnitude increase beyond the Courant condition limit is found to apply. Clearly accuracy in pseudo-time is more important here in the sense of the bearing it has on the development rate to the steady state. In all instances considered, a high level of confidence may be expressed in the schemes suggested so far if equivalent steady state solutions are computed from both explicit and implicit variants.

Numerical results for the implicit scheme

This subsection concentrates on the results for the cavity flow case (a) problem under the implicit scheme. This is described through the developing time histories of the variables at selected domain points and the relative error norm plots throughout the evolutionary process to the steady state.

Low-Re range. The results for $Re = 1$ are presented in Figure 6–8. The value of Δt is now comparable with that of the $Re = 400$ case. This is an acceptable value and is competitive with conventional schemes. The complete removal of step 3 has a marked oscillatory effect on the solution which is again particularly significant in the pressure.

The omission of the extra term at step 3 also has a marked effect on stability which is here reflected in both velocity and pressure relative error norms. The vastly improved development in solution history is particularly significant as can be observed from Figures 6(a) and 6(b). This improvement over the alternative version with the inclusion of this extra term is observed in all variables and throughout the evolutionary period.

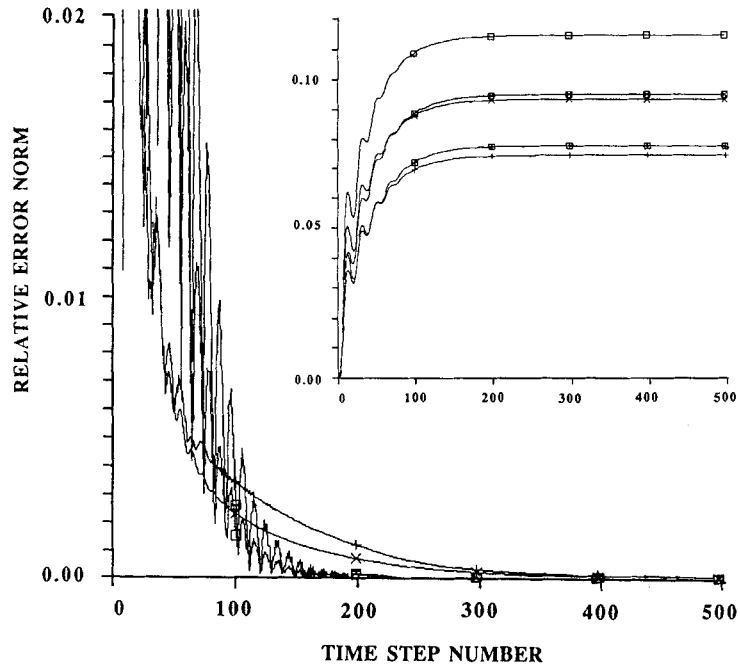

Figure 6(a). Effect of 'extra term' present at stage 3: implicit (+) ($Re = 1$, $\Delta t = 0{\cdot}01$, 5 iterations)

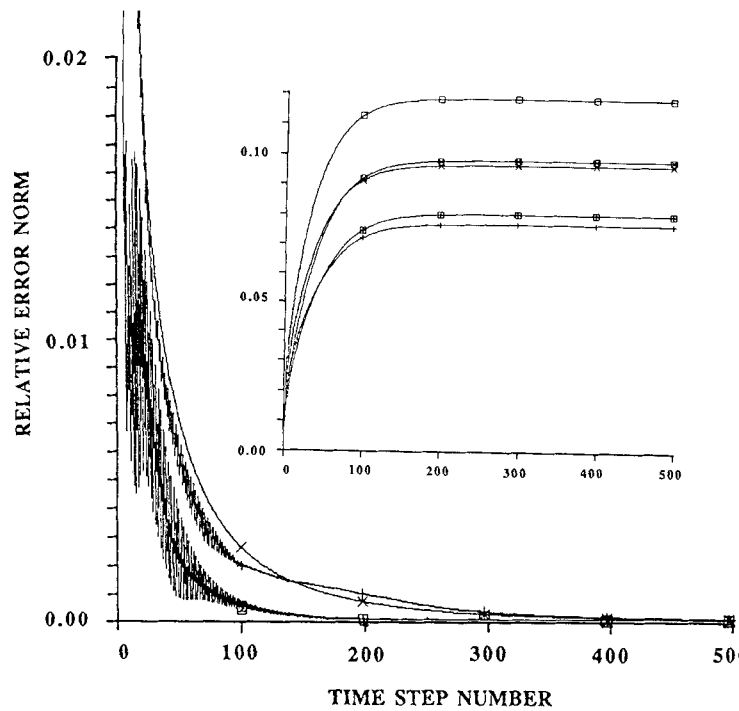

Figure 6(b). Effect of 'extra term' absent at stage 3: implicit (−) ($Re = 1$, $\Delta t = 0{\cdot}01$, 5 iterations)

From Figures 6(b) and 8(b) one can discern the effects of halving the time step at a fixed number of mass iterations, which significantly reduces the magnitude of the relative error norms in both velocity and pressure (though note the curious effect of increased fluctuations in the start-up phase). This same effect is observed on increasing the number of mass iterations from three to five at a fixed time step. The best choice here appears to be $\Delta t = 0{\cdot}01$ and five mass iterations, and these settings correspond to the best solution computed in this case to date. The steady state solution is presented in Figures 7(a) and 7(b) for all variables as before for problem cases (a) and (b) respectively. These low-*Re* results are graphically indistinguishable from those derived for the explicit scheme. The corresponding tabulations of vortex centre strength and position, and

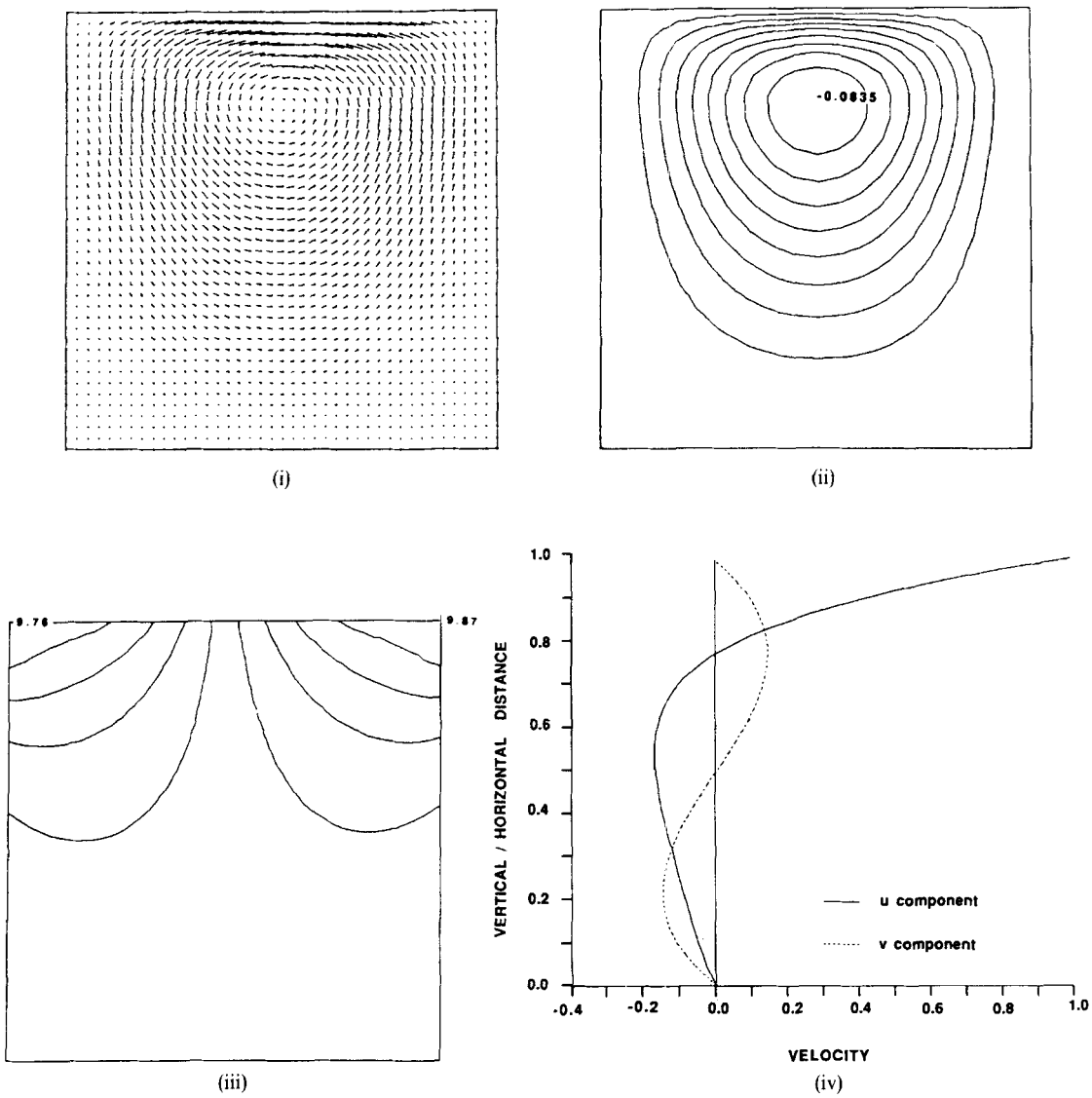

Figure 7(a). Steady state solution case (a): $Re = 1$, $\Delta t = 0{\cdot}01$, 5 iterations, implicit (−) scheme. (i) Velocity field; (ii) streamfunction contours; (iii) pressure contours; (iv) velocity profiles ($u(0{\cdot}5, y)$ and $v(x, 0{\cdot}5)$)

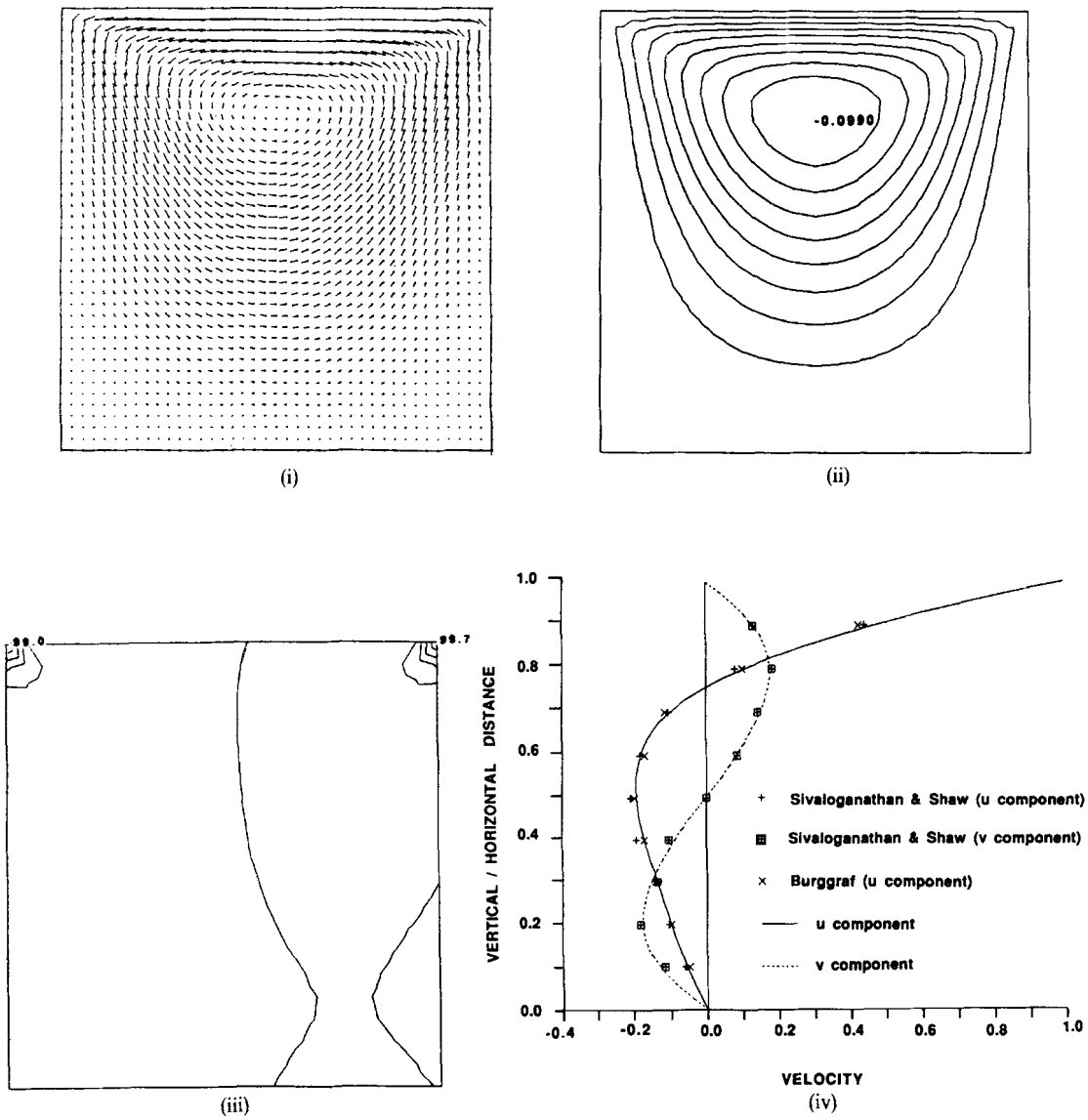

Figure 7(b). Steady state solution case (b): $Re = 1$, $\Delta t = 0{\cdot}01$, 5 iterations, implicit (−) scheme. (i) Velocity field; (ii) streamfunction contours; (iii) pressure contours; (iv) velocity profiles ($u(0{\cdot}5, y)$ and $v(x, 0{\cdot}5)$)

velocity component maxima on the cavity centrelines are provided in Tables II(a) and II(b). These results are seen to compare favourably with the literature.

The effects of altering the number of mass iterations can be clearly observed in Figure 8 where again scale discrepancies are used to reflect the overall requirements to achieve the steady state. Stability is enhanced for the one-iteration or mass-lumping option, but the price paid is in the relatively slow solution development over a fixed time lapse period. This enhancement in stability takes the form of a smoothing out of the high-frequency oscillations present in the relative error norm plots. A 90% development to the steady state is observed over 250 time steps. The same

Table IIa. Comparison of steady state solution against the literature: case (a), $Re = 1$

Scheme	h	ψ_{vc}	Vortex centre	$U_{max}(0{\cdot}5, y)$	$V_{max}(x, 0{\cdot}5)$	$V_{min}(x, 0{\cdot}5)$
Explicit	0·05	0·0825	(0·50, 0·80)	0·177	0·140	−0·138
Explicit	0·10	0·0824	(0·50, 0·80)	0·175	0·168	−0·168
Implicit	0·05	0·0835	(0·50, 0·80)	0·175	0·140	−0·138
Implicit	0·10	0·0841	(0·50, 0·80)	0·183	0·146	−0·146
Reference 31	0·06	0·084	(0·50, 0·80)	—	—	—

Table IIb. Comparison of steady state solution against the literature: case (b), $Re = 1$

Scheme	h	ψ_{vc}	Vortex centre	$U_{max}(0{\cdot}5, y)$	$V_{max}(x, 0{\cdot}5)$	$V_{min}(x, 0{\cdot}5)$
Explicit	0·050	0·0953	(0·50, 0·75)	0·199	0·158	−0·158
Implicit	0·050	0·0990	(0·50, 0·75)	0·199	0·177	−0·177
Reference 39	0·050	0·0995	(0·50, 0·75)	—	—	—
Reference 37	0·0083	0·10006	(0·50000, 0·76667)	—	—	—
Reference 33*	0·050	0·0992	(0·50, 0·75)	—	—	—
Reference 33*	0·025	0·0998	(0·50, 0·76)	0·210	—	—
Reference 40*	0·010	0·1	(0·50, 0·76)	—	—	—
Reference 31*	0·031	0·095	(0·50, 0·78)	—	—	—
Reference 35*	0·05	—	(0·5, 0·75)	0·207	0·138	−0·138
Reference 41*	0·100	—	(0·50, 0·76)	0·200	—	—
Reference 38	0·015	1·00	(0·50, 0·77)	0·188	0·175	−0·175

* $Re = 0$.

final steady state is always reached, but here the five-iteration option is the most cost-effective. This choice achieves a steady state in almost half the number of time steps of the three-iteration case, and within a fifth of that for the mass-lumping alternative.

High-Re range. The results for $Re = 400$ are as depicted for the explicit algorithm with no appreciable differences being observed for the term exclusion at step 3. The complete omission of the third fractional step is reflected in Figure 9 where again oscillatory and decaying fluctuations in the pressure relative error norms are found. Note however that the amplitude and frequency of these fluctuations have increased here over those observed for the explicit algorithm at $Re = 400$.

The effects of altering the number of mass iterations from five to one has the same response as before. The smoother development in solution history of the one-iteration case must be balanced against the reduction in magnitude of the solution attained over a fixed number of time steps. The one-iteration case over 250 time steps provides only a 60% development of the equivalent five- or three-iteration versions. It must be pointed out however that beyond the start-up phase there is little effect on the magnitude of the relative error norm plots here with changes in the mass iteration number, though larger fluctuations are observed at the higher-iteration-number cases in the early phase as before. All the indications are that the three-iteration option is preferable in this instance. Furthermore, changes in Δt proved to have only minor influence on scheme performance, though a value of $\Delta t = 0{\cdot}02$ did render a 10% more rapid development of the solution history against the smaller value of $\Delta t = 0{\cdot}01$. Hence the preference for the larger time step.

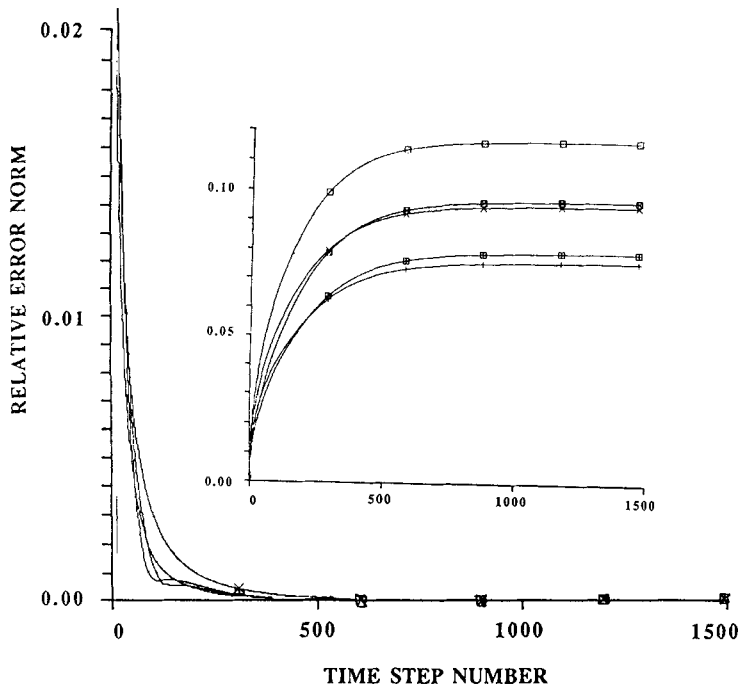

Figure 8(a). Effect of mass iteration number: $Re = 1$, $\Delta t = 0{\cdot}02$, 1 iteration, implicit (−) scheme

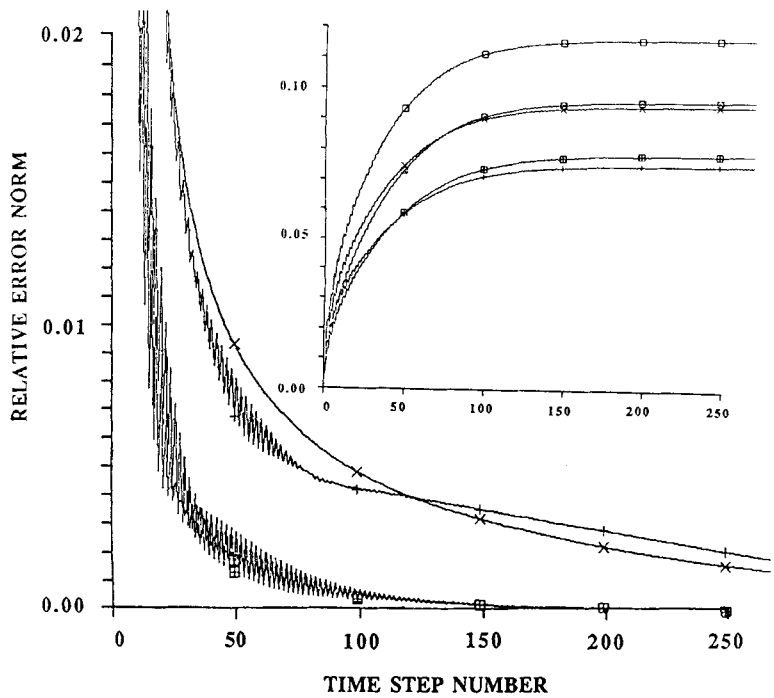

Figure 8(b). Effect of mass iteration number: $Re = 1$, $\Delta t = 0{\cdot}02$, 5 iterations, implicit (−) scheme

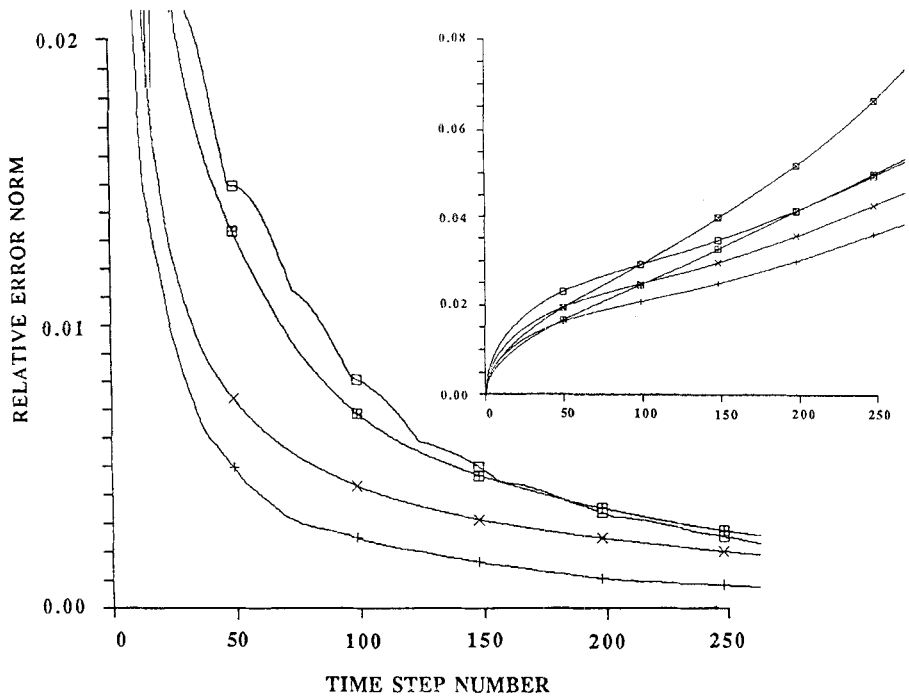

Figure 9(a). Effect of stage 3: present ($Re = 400$, $\Delta t = 0{\cdot}02$, 3 iterations, implicit (−) scheme)

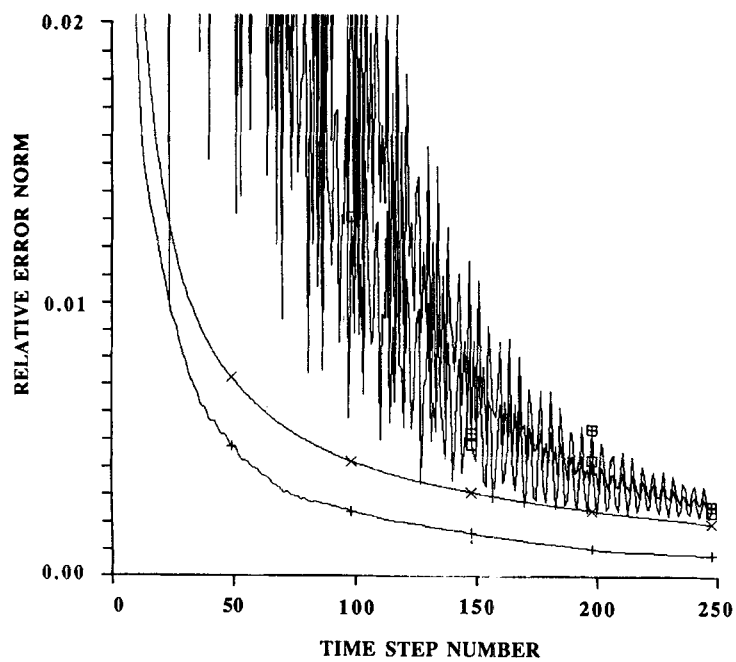

Figure 9(b). Effect of stage 3: removed ($Re = 400$, $\Delta t = 0{\cdot}02$, 3 iterations, implicit (−) scheme)

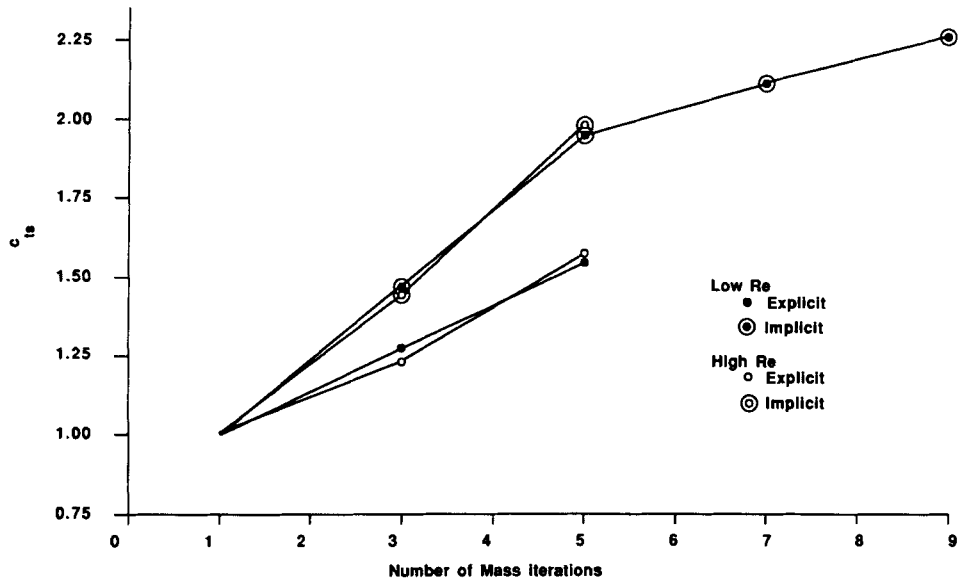

Figure 10(a). Relative cost/time step against number of mass iterations

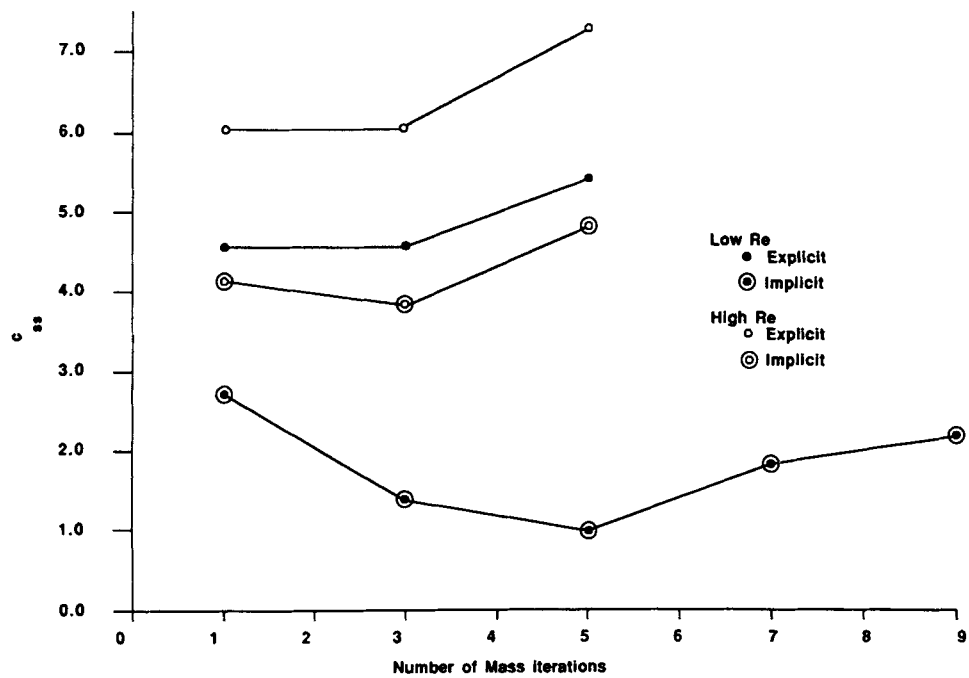

Figure 10(b). Relative run-time cost to reach steady state against number of mass iterations

As noted earlier for low *Re*, there again appears to be little difference between the steady states reached when either the implicit or explicit scheme is employed. The permissible order of Δt is the same, as is the time lapse to the steady state for both approaches. This is in accordance with expectation since at high *Re* values the dominating numerical influence on the left-hand side of the equations is due to the mass matrix terms common to both implicit and explicit schemes.

Run-time costs

Figure 10 is included to provide comparative evidence of the run-time costs and relative efficiencies of the variety of schemes discussed throughout this paper for the various implementation choices. Figure 10(a) shows the cost/time step (c_{ts}) and Figure 10(b) the relative total run-time cost to achieve the steady state (c_{ss}) for each scheme variant. From Figure 10(a) it is apparent that for the mass-lumping option c_{ts} is identical for all schemes, but thereafter grows with the iteration number. Also c_{ts} is always larger in the implicit case and the disparity from the explicit case grows with increasing iteration number. Figure 10(b) permits the identification of scheme optimality. Of particular significance is that the implicit scheme always outperforms the explicit scheme in both high- and low-*Re* ranges. At high *Re* the implicit scheme is 33% more efficient than the explicit form, whilst at low *Re* the corresponding figure is about 80% in favour of the implicit scheme. This is surely convincing evidence of the potential advantages offered by this new implicit scheme.

CONCLUSIONS

The viability has been demonstrated of a Taylor–Galerkin-based finite element technique for solving viscous incompressible flows over a wide range of inertial conditions. This technique will form the basis of a major future research programme, providing a powerful and flexible tool to analyse transient three-dimensional flows of Newtonian and non-Newtonian fluids.

A semi-implicit scheme is now advocated that performs well for $1 \leq Re \leq 400$ on standard benchmark problems. From the theoretical and the numerical standpoint this method is found to be stable, reliable and feasible for large-scale problems. Various sources of instability have been identified in the developmental process of the present scheme and appropriate corrective actions have been taken. These include the effects of modifications to the algorithm at the third fractional step. Furthermore, some conclusions are drawn concerning certain variations in the iterative solution of the Galerkin mass matrix equations. Some attention has also been given here to extracting parallelism from the proposed algorithms with a view to taking advantage of the variety of modern computer architectures available today.

REFERENCES

1. P. Townsend and M. F. Webster, 'An algorithm for the three-dimensional transient simulation of non-Newtonian fluid flows', in G. N. Pande and J. Middleton (eds), *Transient/Dynamic Analysis and Constitutive Laws for Engineering Materials, Vol. II (Proc. Int. Conf. on Numerical Methods in Engineering: Theory and Applications, NUMETA 1987*, Swansea), Nijhoff, Dordrecht, 1987.
2. J. P. Benqué, J. Cahouet, J. Goussebaïlé and A. Haugel, 'Splitting up techniques for computations of industrial flows', in K. W. Morton and M. J. Baines (eds), *Numerical Methods for Fluid Dynamics, Vol. II*, Clarendon Press, Oxford, 1986, pp. 103–128.
3. N. S. Wilkes, C. P. Thompson, J. R. Knightley, I. P. Jones and A. D. Burns, 'On the numerical solution of 3D-incompressible flow problems', in K. W. Morton and M. J. Baines (eds), *Numerical Methods for Fluid Dyanamics, Vol. II*, Clarendon Press, Oxford, 1986, pp. 499–512.
4. R. Peyret and T. D. Taylor, *Computational Methods for Fluid Flow*, Springer-Verlag, New York, 1983.
5. J. van Kan, 'A second-order accurate pressure-correction scheme for viscous incompressible flow', *SIAM J. Sci. Stat. Comput.*, **7**, 870–891 (1986).
6. J. Donea, 'A Taylor–Galerkin method for convective transport problems', *Int. j. numer. methods eng.*, **20**, 101–119 (1984).

7. R. Löhner, K. Morgan and O. C. Zienkiewicz, 'The solution of non-linear hyperbolic equation systems by the finite element method', *Int. j. numer. methods fluids*, **4**, 1043–1063 (1984).
8. R. D. Richtmeyer and K. W. Morton, *Difference Methods for Initial Value Problems*, 2nd edn, Wiley, New York, 1967.
9. K. W. Morton, 'Initial-value problems by finite difference and other methods', in D. Jacobs (ed.), *Proc. Conf. IMA 'State of the Art in Numerical Analysis'*, York, April 1976, Academic Press, New York, 1977.
10. A. N. Brooks and T. J. R. Hughes, 'Streamline upwind/Petrov–Galerkin formulations for convection dominated flows with particular emphasis on the incompressible Navier–Stokes equations', *Comput. Methods Appl. Mech. Eng.*, **32**, 199–259 (1982).
11. L. Quartapelle, 'Vorticity conditioning in the computation of two-dimensional viscous flows, *J. Comput. Phys.*, **40**, 453–477 (1981).
12. P. M. Gresho and S. T. Chan, 'A new semi-implicit method for solving the time-dependent conservation equations for incompressible flow', in *Numerical Methods in Laminar and Turbulent Flow*, Pineridge Press, Swansea, 1985, pp. 3–21.
13. J. Donea, S. Giuliani, H. Laval and L. Quartapelle, 'Finite element solution of the unsteady Navier–Stokes equations by a fractional step method', *Comput. Methods Appl. Mech. Eng.*, **30**, 53–73 (1982).
14. A. J. Chorin, 'Numerical solution of the Navier–Stokes equations', *Math. Comput.*, **22**, 745–762 (1968).
15. R. Temam, 'Sur l'approximation de la solution de Navier–Stokes par la méthode des pas fractionnaires', *Arch. Rat. Mech. Anal.*, **32**, 135–153 (1969).
16. R. I. Issa, 'Solution of the implicitly discretised fluid flow equations by operator-splitting', *J. Comput. Phys.*, **62**, 40–65 (1986).
17. C. Cuvelier, A. Segal and A. A. van Steenhoven, *Finite Element Methods and Navier–Stokes Equations*, D. Reidel, Dordrecht, 1986.
18. P. M. Gresho, R. L. Lee and R. L. Sani, 'Advection-dominated flows with emphasis on the consequences of mass lumping', in *Finite Elements in Fluids, Vol. 3*, Wiley, New York, 1978, pp. 745–756.
19. K. W. Morton, 'Galerkin finite element methods and their generalisations', *Oxford University Computer Laboratory, N.A. Report 6*, 1986 (invited lecture at *Conf. IMA 'State of the Art in Numerical Analysis'*, Birmingham, April 1986).
20. K. W. Morton, E. E. Süli and A. Priestley, 'A stability analysis of the Lagrange–Galerkin method with non-exact integration', *Oxford University Computer Laboratory, N.A. Report 14*, 1986.
21. G. Strang and G. J. Fix, *An Analysis of the Finite Element Method*, Prentice-Hall, Englewood Cliffs, NJ, 1973.
22. R. Löhner, K. Morgan and O. C. Zienkiewicz, 'The use of domain splitting with an explicit hyperbolic solver', *Comput. Methods Appl. Mech. Eng.*, **45**, 313–329 (1984).
23. J. H. Wilkinson and C. Reinsch, *Handbook for Automatic Computation, Vol. II, Linear Algebra*, Springer-Verlag, New York, 1971, pp. 50–56.
24. A. V. Aho, J. E. Hopcroft and J. D. Ullman, *The Design and Analysis of Computer Algorithms*, Addison-Wesley, Reading, MA, 1974.
25. A. J. Wathen, 'Realistic eigenvalue bounds for the Galerkin mass matrix', *IMA J. Numer. Anal.*, **7**, 449–457 (1987).
26. O. C. Zienkiewicz, K. Morgan, J. Peraire, M. Vandati and R. Löhner, 'Finite elements for compressible gas flow and similar systems', paper presented at *7th Int. Conf. on Computer Methods and Applications in Science and Engineering*, Versailles, December 1985.
27. J. R. Westlake, *A Handbook of Numerical Matrix Inversion and Solution of Linear Equations*, Wiley, New York, 1968.
28. L. A. Hageman and D. M. Young, *Applied Iterative Methods*, Academic Press, London, 1981.
29. J. Donea, S. Giuliani, H. Laval and L. Quartapelle, 'Time-accurate solution of advection–diffusion problems by finite elements', *Comput. Methods Appl. Mech. Eng.*, **45**, 123–145 (1984).
30. N. Levine, 'Superconvergent estimation of the gradient from linear finite element approximations on triangular elements', *University of Reading, N.A. Report 3*, 1985.
31. M. Bourcier and C. François, 'Intégration numérique des équations de Navier–Stokes dans un domain carré', *Recherche Aerospatiale*, **131**, 23–33 (1969).
32. P. Bontoux, 'Contribution à l'étude des écoulements visqueux en milieu confiné', *Thèse Doctorat d'Etat*, IMFM, Université d'Aix–Marseille, 1978.
33. O. R. Burggraf, 'Analytical and numerical studies of the structures of steady separated flows', *J. Fluid. Mech.*, **24**, 113–151 (1966).
34. D. W. Pepper and R. E. Cooper, 'Numerical solution of recirculating flow by a simple finite element recursion relation', *Comput. Fluids*, **8**, 213–223 (1980).
35. M. Nallasamy and K. Krishna Prasad, 'On cavity flow at high Reynolds number', *J. Fluid Mech.*, **79**, 391–414 (1977).
36. Hwar-Ching Ku and D. Hatziauramidis, 'Solutions of the two-dimensional Navier–Stokes equations by Chebyshev expansion methods', *Comput. Fluids*, **13**, 99–113 (1985).
37. R. Schreiber and H. B. Keller, 'Driven cavity flows by efficient numerical techniques', *J. Comput. Phys.*, **49**, 310–333 (1983).
38. S. Sivaloganathan and G. J. Shaw, 'A multigrid method for recirculating flows', *Int. j. numer. methods fluids*, **8**, 417–440 (1988).
39. M. M. Gupta and R. P. Manohar, 'Boundary approximations and accuracy in viscous flow computations', *J. Comput. Phys.*, **31**, 265–288 (1979).
40. F. Pan and A. Acrivos, 'Steady flows in rectangular cavities', *J. Fluid Mech.*, **28**, 643–655 (1967).
41. M. Kawaguti, 'Numerical solution of the Navier–Stokes equations for the flow in a two-dimensional cavity', *J. Phys. Soc. Japan*, **16**, 2307–2315 (1961).